of PMe_3 was essentially thermoneutral relative to the reactants. The trans isomer of PtP_2H_2 was 4 kcal/mol more stable than the cis form for P = PH_3 and 23 kcal/mol more stable for P = PMe_3. CI calculations on the $Pt(PH_3)_2H_2$ species showed only slight differences in the reaction barrier and reaction energy.

A C_{2v} transition state with symmetric Pt-H bonds was found, and no evidence was uncovered to support less symmetric pathways. At the transition state a significant H-H interaction is still retained, and only at later stages of the reaction does the incorporation of Pt^+-H^- character disrupt the H_2 bond. The large barrier obtained for reductive elimination of H_2 from the cis dihydride was discussed in view of the apparent instability of cis dihydride complexes.

Acknowledgment. This research was carried out under the auspices of the U.S. Department of Energy. We thank Professor James Ibers for initially interesting us in platinum phosphine species and Professor Roald Hoffmann for an advance copy of the paper regarding the reductive elimination of metal alkyls.

Note Added in Proof. Recently Paonessa and Trogler[46] have actually observed the cis dihydrides PtP_2H_2 (P = PEt_3) in striking confirmation of their predicted stabilities here. These compounds, which represent the first known cis dihydrides of Pt with sterically unhindered ligands, are found to be in solvent-assisted equilibrium with the trans isomer.

Registry No. H_2, 1333-74-0; $Pt(PH_3)_2$, 76830-85-8; $Pt[P(CH_3)_3]_2$, 82209-22-1; *cis*-$Pt(PH_3)_2H_2$, 76832-29-6; *trans*-$Pt(PH_3)_2H_2$, 76830-84-7; *cis*-$Pt[P(CH_3)_3]_2H_2$, 80540-35-8; *trans*-$Pt[P(CH_3)_3]_2H_2$, 80581-71-1.

(46) Paonessa, R. S.; Trogler, W. C. *J. Am. Chem. Soc.* **1982**, *104*, 1138.

Nature of Dilute Solutions of Sodium and Methoxide Ions in Methanol[1]

William L. Jorgensen,*[2] Bernard Bigot,[3] and Jayaraman Chandrasekhar

Contribution from the Department of Chemistry, Purdue University, West Lafayette, Lafayette, Indiana 47907. *Received September 25, 1981*

Abstract: Monte Carlo statistical mechanics simulations have been carried out for Na^+ and CH_3O^- in liquid methanol at 25 °C and 1 atm. The intermolecular interactions were described by Lennard-Jones and Coulomb terms in the TIPS format. Detailed information on the structures and thermodynamics of the solutions has been obtained. The computed heats and volumes of solution are in accord with available experimental data. For Na^+ in methanol, the coordination number is found to be 6, while CH_3O^- has about five solvent molecules near the oxygen. Beyond the first solvent shells the influence of the ions is much diminished. In particular, analyses of the hydrogen bonding do not show evidence for significant structure broken regions in the solutions. Rather the ions plus their first solvent shells interface readily into the bulk solvent. An interesting prediction is that the first two solvent shells around sodium ion contain the same number of methanol molecules. Although this contrasts conventional ideas about solvation, it is a consequence of the substantial compression of the first solvent shell.

I. Introduction

Much attention has been paid to the thermodynamics and structure of aqueous solutions of electrolytes because of their importance in electrochemistry and biochemistry.[4] In comparison, nonaqueous salt solutions have received limited study;[5] particularly little is known about their structure since diffraction experiments analogous to those for aqueous solutions have not yet been undertaken.[6] Nevertheless, nonaqueous solutions are of paramount importance in organic chemistry since they are the principal reaction media. There is no doubt that the predictive abilities of synthetic organic chemists could be enhanced by a greater understanding of the solvation of substrates and intermediates in solution. In view of the importance of solvent effects on reactivity,[5c,d] it is ultimately desirable to discuss reactions not largely as they are now in terms of isolated reactants, but rather with knowledge of the solvation and aggregation of the species and how these factors vary along reaction paths. To this end, an extensive program for the theoretical study of organic chemistry in solution has been undertaken in our laboratory. The initial work has centered on Monte Carlo statistical mechanics simulations of common organic solvents including alcohols,[7] ethers,[8] hydrocarbons,[9,10] and alkyl chlorides.[10] An important development was the generation of a set of transferable intermolecular potential functions (TIPS) that yield good structural and thermodynamic results for these liquids.[7-11] In particular, the computed densities are within 0-6% of experimental values from 1 to 15000 atm near room temperature.[7-12] Furthermore, detailed insights into the structures of the liquids have been obtained via stereoplots and numerous distributions for atomic positions, energetics, conformations, coordination numbers, and hydrogen bonding.

Now that the theoretical approach has been validated for pure liquids, attention is being turned to dilute solutions of neutral molecules and ions. An initial study described here is for sodium ion and methoxide ion in methanol. This system was chosen since

(1) Quantum and Statistical Mechanical Studies of Liquids 21.
(2) Camille and Henry Dreyfus Foundation Teacher-Scholar, 1978-1983: Alfred P. Sloan Foundation Fellow, 1979-1981.
(3) On leave from the Université Pierre et Marie Curie and Ecole Normale Supérieure de Saint Cloud, France; CNRS-NSF Fellow, 1980-1981.
(4) For reviews, see: (a) "Water, A Comprehensive Treatise"; Franks, F., Ed.; Plenum Press: New York, 1973; Vol. 3. (b) Desnoyers, J. E.; Jolicoeur, C. In "Modern Aspects of Electrochemistry"; Bockris, J. O'M., Conway, B. E., Eds.; Plenum Press: New York, 1969; Vol. 5, p 1.
(5) For reviews, see: (a) Padova, J. In "Water and Aqueous Solutions"; Horne, R. A., Ed.; Wiley-Interscience: New York, 1973; p 109. (b) Garst, J. F. In "Solute-Solvent Interactions"; Coetzee, J. F., Ritchie, C. D., Eds.; Marcel Dekker: New York, 1969; p 539. (c) Abraham, M. H. *Prog. Phys. Org. Chem.* **1974**, *11*, 1. (d) Parker, A. J. *Chem. Rev.* **1969**, *69*, 1.
(6) Neilson, G. W.; Enderby, J. E. *Annu. Rep. Prog. Chem., Sect. C* **1979**, *76*, 185.
(7) (a) Jorgensen, W. L. *J. Am. Chem. Soc.* **1981**, *103*, 341, 345. (b) Jorgensen, W. L.; Ibrahim, M. *Ibid.* **1982**, *104*, 373.
(8) Jorgensen, W. L.; Ibrahim, M. *J. Am. Chem. Soc.* **1981**, *103*, 3976.
(9) Jorgensen, W. L. *J. Am. Chem. Soc.* **1981**, *103*, 4721.
(10) (a) Jorgensen, W. L. *J. Am. Chem. Soc.* **1981**, *103*, 677. (b) Jorgensen, W. L.; Binning, R. C.; Bigot, B. *Ibid.* **1981**, *103*, 4393. (c) Jorgensen, W. L.; Bigot, B. *J. Phys. Chem.*, in press.
(11) Jorgensen, W. L. *J. Am. Chem. Soc.* **1981**, *103*, 335.
(12) The density of liquid water at 25 °C and 1 atm has also been computed recently with the TIPS reported for water in ref 11. The computed value (0.996 ± 0.006 g cm^{-3}) is in exact agreement with experiment. Better accord for other properties of water is obtained with the TIPS2 potential (Jorgensen, W. L. *J. Chem. Phys.*, in press).

0002-7863/82/1504-4584$01.25/0

sodium methoxide in methanol is a commonly used base for proton transfer, substitution, elimination, and addition reactions. It also permits the analysis of the structures of the solutions for a prototype organic anion and alkali cation in an important organic solvent. Although Monte Carlo and molecular dynamics calculations have been performed for alkali, ammonium, and halide ions in water,[13-15] to our knowledge no simulations have previously treated ions in a nonaqueous molecular liquid. In fact, there is even a lack of qualitative models for nonaqueous solutions. Whether the useful, three-region description of Frank and Wen[16] for aqueous solutions remains valid in other solvents is considered below. The detailed nature of the calculations permits other fundamental issues to be addressed such as the concept of solvation shells, the range of influence of an ion on the solvent's structure, and structure-making and structure-breaking in a nonaqueous medium.

To begin, a summary of the potential functions and computational details for the fluid simulations is presented. This is followed by the results and discussion.

II. Statistical Mechanics

A. Simulations of Dilute Solutions. The Monte Carlo calculations were carried out for systems of one ion and 127 solvent molecules in a cube with periodic boundary conditions. This attempts to mimic a very dilute solution, though the correspondence is not exact in view of the additional images of the ion and the absence of counterions. It should be noted that the solvent molecules only interact with the ion in the central cell, although some effects on the solvent's structure near the edges of the periodic cube might be anticipated owing to the images of the ion in adjacent cells. As shown below, these edge effects do not appear to be significant for systems of the present size since the structure and properties of the solvent in the periphery of the cube away from the ions are the same as for the pure liquid. Similar boundary conditions were used in the recent Monte Carlo simulations of alkali and halide ions in water by Mezei and Beveridge.[14]

The present simulations were performed in the isothermal–isobaric (NPT) ensemble at 25 °C and 1 atm. This is the preferred ensemble for such studies since it corresponds to the usual experimental conditions. Nevertheless, the NPT ensemble has received little use owing to its somewhat greater demands on computer time (ca. 15% more than Monte Carlo calculations in the canonical (NVT) ensemble) and to the concern that the available intermolecular potential functions might not yield reasonable computed densities. The latter problem has been overcome with our TIPS which have been used in NPT simulations for liquid water,[12] methanol,[7b] dimethyl ether,[8] THF,[17] *n*-butane,[9] and 1,2-dichloropropane.[10c] The largest error in the computed densities for these cases, which included pressures up to 15 000 atm for *n*-butane and methanol, is 5.6%.

Summaries of the formalism and general computational procedure for Monte Carlo calculations in the NPT ensemble may be found elsewhere.[8,9,18] However, some details concerning the present simulations need to be mentioned. First of all, dilute solution simulations cause statistical problems due to the low solute concentration relative to the solvent. If the solute and solvent molecules are moved randomly to generate new configurations, the statistics for the solute will be less by a factor of ca. 100 than for the solvent. To help remedy this problem, Owicki and Scheraga proposed techniques to increase the sampling of the solute and its nearest neighbors.[19] As discussed previously,[20a] we have found the preferential sampling procedure in which the probability of moving a solvent molecule is proportional to $1/r^2$, where r is the distance from the solute to the solvent molecule, to be valuable.[19b] However, $1/r^2$ sampling proved too severe in the present cases because of the relatively short ion–solvent distances for the first solvent shell; too little sampling of the outer solvent molecules occurred which causes slow equilibration and expansion of the system using normal frequencies for volume moves. Consequently, $1/(r^2 + c)$ sampling was tested and found to be appropriate with values for the constant, c, of 60–70 Å^2. This enhances moving the solute's nearest neighbors over the outermost solvent molecules by a factor of 4–5 which appears to be the upper limit to still allow adequate solvent equilibration. Furthermore, the sampling of the solute was augmented by a factor of 3–4 over random sampling by attempting to move it every 30–40 configurations. In summary, the present simulations employed both Metropolis and $1/(r^2 + c)$ preferential sampling.

The initial configurations for the dilute solutions were obtained by modifying configurations from the NPT simulation of pure liquid methanol at 25 °C and 1 atm which used the TIPS.[7b] The latter calculation forms a basis for comparison of the dilute solution results with the pure solvent. Since the simulation of pure methanol involved 128 monomers, one near the center of the periodic cube was replaced by an ion. Unusually long equilibration periods of 2000–5000K configurations then ensued as the preferential sampling procedures and convergence characteristics of the simulations were studied. Final averaging was performed over an additional 1600K configurations for the methoxide solution and 2000K for sodium ion. Beveridge et al. have also recently studied the convergence of Monte Carlo simulations for aqueous solutions of similar size.[20b] They too found that adequate statistics for the solute can be obtained by averaging over about 2000K when preferential sampling is used.

For both systems spherical cutoffs at 10 Å were invoked in evaluating the intermolecular potential functions (vide infra) which included interactions with a monomer's ca. 60 nearest neighbors. New configurations were generated by translating the selected monomer in all three Cartesian directions and by rotating it about a randomly selected Cartesian axis (except for Na^+). The volume moves involved scaling all the intermolecular distances and were attempted on every 600th configuration. Acceptance rates of 40–50% were maintained by using ranges of ±0.17 Å for the translations, ±17° for the rotations, and ±190 Å^3 for the volume moves.

The computations were run in part on the CDC/6600 system at the Purdue University Computing Center and primarily on a Harris Corp. H-80 computer in our laboratory. Roughly 250K configurations can be run per day on the H80.

B. Potential Functions. The solvent–solvent and solvent–solute interactions were described in the TIPS format. The parameters previously reported for alcohols were used in this work.[7,11] Each methanol monomer is represented by three interaction sites centered on the carbon, oxygen, and hydroxyl hydrogen with the methyl hydrogens implicit. The bond lengths and angle are fixed in the methanol monomers at standard values: r(OH) = 0.945 Å, r(CO) = 1.430 Å, and ∠COH = 108.5°.[11] Interaction energies, ϵ_{mn}, are determined by the intermolecular interactions between the sites including Lennard-Jones and Coulomb terms (eq 1). The

$$\epsilon_{mn} = \sum_{i}^{\text{on } m} \sum_{j}^{\text{on } n} \left(\frac{q_i q_j e^2}{r_{ij}} + \frac{A_i A_j}{r_{ij}^{12}} - \frac{C_i C_j}{r_{ij}^{6}} \right) \qquad (1)$$

q, A, and C parameters have been chosen to yield good results for the geometries and interaction energies of gas-phase complexes in comparison with experiment or high-quality ab initio quantum mechanical results and to provide reasonable thermodynamic and structural descriptions of liquids.[7-12] In particular, Monte Carlo results for liquid methanol and ethanol using the TIPS are in good agreement with experimental thermodynamic and structural data including diffraction results.[7] The greatest discrepancy for the thermodynamics is the roughly 15% underestimation of heats of vaporization for hydrogen-bonded liquids. This may by attrib-

(13) From, J.; Clementi, E.; Watts, R. O. *J. Chem. Phys.* **1975**, *62*, 1388. Watts, R. O. *Mol. Phys.* **1976**, *32*, 659.
(14) Mezei, M.; Beveridge, D. L. *J. Chem. Phys.* **1981**, *74*, 6902.
(15) Palinkas, G.; Riede, W. O.; Heinzinger, K. *Z. Naturforsch., Teil A* **1977**, *32*, 1137. Szasz, G. I.; Heinzinger, K. *Ibid.* **1979**, *34*, 840. Szasz, G. I.; Riede, W. O.; Heinzinger, K. *Ibid.* **1979**, *34*, 1083.
(16) Frank, H. S.; Wen, W.-Y. *Discuss. Faraday Soc.* **1957**, *24*, 133.
(17) Chandrasekhar, J.; Jorgensen, W. L., submitted for publication.
(18) Owicki, J. C.; Scheraga, H. A. *J. Am. Chem. Soc.* **1977**, *99*, 7403.
(19) (a) Owicki, J. C.; Scheraga, H. A. *Chem. Phys. Lett.* **1977**, *47*, 600. (b) Owicki, J. C. *ACS Symp. Ser.* **1978**, No. 86, 159.
(20) (a) Bigot, B.; Jorgensen, W. L. *J. Chem. Phys.* **1981**, *75*, 1944. (b) Mehrotra, P. K.; Mezei, M.; Beveridge, D. L. *Ibid.*, submitted for publication.

Table I. TIPS Parameters for Na^+, CH_3O^- and CH_3OH[a]

site	q	$10^{-3}A^2$	C^2
O in CH_3OH	−0.685	515	600
CH_3 in CH_3OH	0.285	7950	2400
H_o in CH_3OH	0.400	0	0
O in CH_3O^-	−0.900	515	2500
CH_3 in CH_3O^-	−0.100	7950	3600
Na^+	1.000	19.6	625

[a] Units are for q (electrons), A^2 (kcal Å^{12}/mol), and C^2 (kcal Å^6/mol). e^2 in eq 1 is 332.177 52 kcal Å/mol.

Table II. TIPS Results for Complexes[a]

complex	parameter	TIPS	ab initio
MeOH···OHMe	r(OO)	2.79	2.95[c]
	θ[b]	27	48[c]
	ΔE	−5.68	−5.66[c]
MeO^-···HOMe	r(OO)	2.57	2.54[d]
	∠CO···H	145	117[d]
	ΔE	−20.2	−25.7[e]
Na^+···OHMe	r(NaO)	2.22	2.11[f]
	∠NaOC	118	127[f]
	ΔE	−26.4	−28.9[g]

[a] Distances in Å, angles in degrees, energies in kcal/mol. [b] θ is the H···OX angle where X is on the bisector of the COH angle in the H-bond acceptor. [c] 6-31G*, ref 22. [d] 4-31G, ref 21. [e] 6-31G*, ref 21. [f] 3-21G, ref 23. [g] 6-31G*, ref 23.

utable to the neglect of three-body effects inherent in the two-body TIPS and/or the need for a correction for the change in vibrational energy upon vaporization which should be particularly significant in hydrogen-bonded liquids.[7,11]

The TIPS parameters for methoxide ion were chosen to provide agreement with our ab initio results for the methoxide–methanol complex since no experimental gas-phase data are available in this case.[21] A general study of RO^-···HOR′ complexes was carried out with R, R′ = H, CH_3.[21] Calculations with the 4-31G basis set yielded reasonable geometries for the complexes in comparison to larger basis set findings. Furthermore, the 6-31G* bonding energy for $H_3O_2^-$ (−34.6 kcal/mol) was computed to be 6 kcal/mol below experimental values. In conjunction with the 6-31G* results for methoxide–methanol,[21] the best estimate for the minimum interaction energy of this pair is then ca. −20 kcal/mol. Thus, the TIPS parameters for methoxide were selected to aim at this value and at the 4-31G geometrical results and to be consistent with other TIPS parameters. Also, the CO distance used in the TIPS for methoxide ion is 1.37 Å which is the 4-31G optimized value found in methoxide–methanol.[21] The resultant TIPS parameters for methoxide anion are summarized in Table I. The A values for CH_3 and O were retained at their alkyl group and alcohol values, while the corresponding C parameters were increased consistent with the greater polarizability of the anion. The negative charge is distributed 90% on oxygen and 10% on the methyl group. These parameters yield the desired outcome for methoxide–methanol as summarized in Table II; the dimerization energy is −20.2 kcal/mol and the OO distance (2.57 Å) is close to the 4-31G value (2.54 Å). The CO^-···H angles differ by nearly 30°, but the potential surfaces are very flat in this region so the discrepancy is not worrisome. The same is true for the angle θ in the methanol dimer (Table II). In this case the 6-31G* value for the OO distance is probably an overestimate.[11]

There are only two parameters for sodium ion since the charge is fixed. Again the parameters were chosen to fit ab initio results. As will be published elsewhere, an extensive ab initio study for complexes of 20 first- and second-row bases with H^+, Li^+, and Na^+ has been carried out.[23] All geometries have been fully optimized at the 3-21G level with subsequent single point 6-31G*

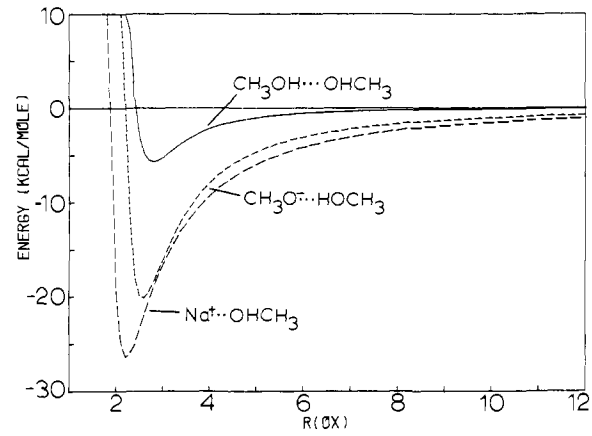

Figure 1. Dependence of the interaction energy on the OO or NaO distance in the indicated complexes. Distances are in Å and energies are in kcal/mol throughout this paper. Angular variables for the complexes have been fixed at their optimal values for the minima.

calculations. The TIPS parameters for Na^+ were selected to provide agreement with the ab initio data for the geometries and interaction energies of its complexes with water, methanol, and dimethyl ether.[23] The resultant parameters are recorded in Table I and the results for the sodium ion-methanol complex are shown to be in reasonable accord with the ab initio findings in Table II. It should also be noted that the TIPS potential surface for Na^+···OH_2 using the original water parameters[11] is nearly identical with the potential surface from Clementi's Hartree–Fock level calculations.[24]

More insight into the potential functions can be obtained by comparing the well shapes for $(MeOH)_2$, MeO^-···HOMe, and Na^+···OHMe as shown in Figure 1. The dependence of the interaction energy on the OO or NaO distance is illustrated with the angular variables fixed at their optimal values for the minima. Clearly, the bonding between individual solvent molecules in the methanolic solutions is far weaker than the potential solute–solvent interactions. Thus, the ions are expected to have a substantial orienting influence on proximate solvent molecules with the more localized sodium ion having the most profound effect.

III. Results and Discussion

A. Thermodynamics. Several thermodyamic quantities can be calculated for the process of transferring the solute from the ideal gas phase into the solvent. The energy of solution is given by eq 2 where the total energy for the solution consists of the solute–

$$\Delta E^\circ_{sol} = E_{SX} + E_{SS} - E^*_{SS} = E_{SX} + \Delta E_{SS} \qquad (2)$$

solvent (E_{SX}) and solvent–solvent (E_{SS}) contributions, E^*_{SS} is the energy of the pure solvent and ΔE_{SS} is the solvent reorganization energy. If intramolecular motions such as internal rotation and vibrations were considered for the solute and solvent molecules, additional terms representing the changes in these quantities would also be needed in eq 2. Next the volume of solution is simply $\Delta V^\circ_{sol} = V - V^*$ where V and V^* are the volume for the solution and pure solvent, respectively. The enthalpy of solution is then $\Delta H^\circ_{sol} = \Delta E^\circ_{sol} + P\Delta V^\circ_{sol} - RT$, where the last term represents the PV contribution for the solute in the ideal gas. In practice, we keep track of the total enthalpy during the simulations, so $\Delta H^\circ_{sol} = H_T - H^*_T - H_X^{ig}$ where the three enthalpies are for the solution, pure solvent, and solute in the ideal gas phase, respectively. For the present cases, the H, E, and V terms correspond to the total figures for 127 solvent molecules and the solute in the solutions and for 127 monomers in the pure solvent. Also, cutoff corrections have been made for the solvent–solvent energies in the usual manner.[7,11] The cutoff correction for the Lennard-Jones part of the solute–solvent interactions is negligible, ca. 0.3 kcal/mol (0.2%). The Coulombic contribution would be more

(21) Jorgensen, W. L.; Ibrahim, M. *J. Comput. Chem.* **1981**, *2*, 7.
(22) Tse, Y. C.; Newton, M. D.; Allen, L. C. *Chem. Phys. Lett.* **1980**, *75*, 350.
(23) Smith, S. F.; Chandrasekhar, J.; Jorgensen, W. L. *J. Phys. Chem.*, in press.
(24) Kistenmacher, H.; Popkie, H.; Clementi, E. *J. Chem. Phys.* **1973**, *59*, 5842.

Table III. Thermodynamic Results for Na^+ and CH_3O^- in Methanol at 25 °C and 1 Atm[a]

property	Na^+	CH_3O^-
E_{SX}	−206 ± 2	−143 ± 1
E_{SS}	−791 ± 7	−830 ± 4
E^*_{SS}	−895 ± 6	−895 ± 6
ΔE_{SS}	105 ± 12	66 ± 9
ΔE°_{sol}	−101 ± 12	−77 ± 9
V	9076 ± 51	9103 ± 47
V^*	9093 ± 67	9093 ± 67
ΔV°_{sol}	−17 ± 118	10 ± 114
ΔV°_{sol}(exptl)	−28 ± 3[b]	21 ± 3[c]
ΔH°_{sol}	−102 ± 12	−78 ± 9
ΔH°_{sol}(exptl)	−111 ± 10[d]	−104 ± 18[c]

[a] E and H in kcal/mol; V in Å^3. Calculated results are total quantities for the ion and 127 solvent molecules. Subscripts SS and SX indicate the solvent-solvent and solvent-solute contributions. Superscript * indicates the pure solvent. [b] Reference 31a. [c] See text. [d] References 4b and 25. Error bars estimated.

significant if the ions still have an orienting influence on the solvent molecules beyond 10 Å. Otherwise, the neutral solvent molecules would be oriented randomly and the Coulombic correction would be negligible. The latter situation appears to prevail (vide infra), so a correction has not been made for the effect.

The results from the simulations are presented in Table III. The error bars ($\pm 2\sigma$) for the computed quantities were obtained from separate averages over each 50K configurations. It is seen that the enthalpies and energies of solution are nearly identical since the $P\Delta V^\circ_{sol}$ term has minor influence at 1 atm. The solute–solvent energy is substantially more attractive for Na^+ than CH_3O^-. Consistently, the Na^+ disrupts the solvent more as reflected by the more positive ΔE_{SS}. Consequently, the ΔH°_{sol} is only 24 kcal/mol more negative for Na^+ than CH_3O^-. In view of the error bars, the computed heats of solution are in accord with the experimental values recorded in Table III. Quantitative agreement could not be expected because of the inexact correspondence of the simulations to an infintely dilute solution, as discussed in section II.A, and to the neglect of three-body effects which could reduce the solute–solvent bonding.[13,14,24] The latter phenomenon is associated with the enhanced polarization of the solvent molecules coordinated to the ion which causes the solvent–solvent interactions between these nearest solvent molecules to be more repulsive than similar interactions in the absence of the ion. In addition, some N dependence due to the periodicity and the cutoff is possible for the energetics. Though this effect is slight for the total energies, it may amount to a much as 15% for the heats of solution based on results for aqueous solutions.[14]

Some discussion of the origin of the experimental single-ion heats of solution at infinite dilution, ΔH°_{sol}, is needed. First, the general paucity of such data for nonaqueous solutions and even for aqueous solutions involving other than atomic or ammonium ions is unfortunate. For Na^+ in methanol, the ΔH°_{sol} for Na^+ in water (−106 kcal/mol)[4b] was combined with the heat of transfer for Na^+ from water to methanol (−4.8 kcal/mol)[25] to give the value reported in Table III. A more circuitous route was needed involving the thermodynamic cycle in Scheme I for methoxide ion in methanol at 25 °C. From the cycle eq 3 is obtained for the

$$\Delta H^\circ_{sol}(CH_3O^-) = \Delta H^{aq}_{ion} + \Delta H^\circ_{sol}(CH_3OH) + \Delta H^\circ_{sol}(OH^-) - \Delta H^g_{ion} + \Delta H^\circ_{vap}(H_2O) \quad (3)$$

heat of solution of methoxide ion in water. The five quantities on the right-hand side of eq 3 have experimental values of −0.7,[26] −10.8,[27] −115 ± 10,[28] 11.6 ± 2,[26] and 10.7 kcal/mol[29] which yield −104 ± 13 for ΔH°_{sol} of CH_3O^- in water. This is dominated by

Scheme I

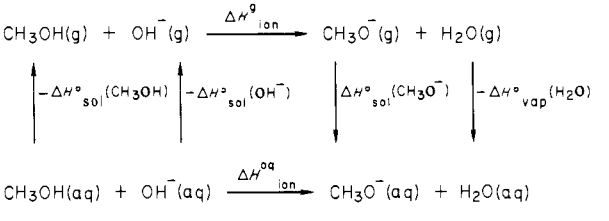

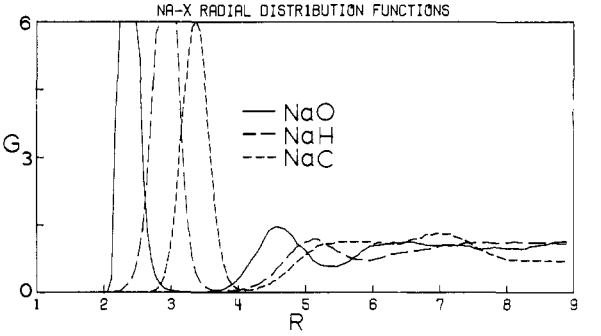

Figure 2. Computed NaO, NaH, and NaC radial distribution functions (rdfs) for Na^+ in methanol.

the heat of hydration for hydroxide ion which has been estimated at −101 and ca. −115 kcal/mol with the lower value being more recent.[4b,28] Finally, a heat of transfer for methoxide ion from water to methanol is needed. Unfortunately, an experimental value is not available; however, ΔH_{tr} is known for Cl^-, Br^-, I^-, ClO_4^-, and BPh_4^-.[25] The values are very similar at 0 ± 2 kcal/mol, so this same value with large error bars has been used to yield the experimental estimate of ΔH°_{sol} for CH_3O^- in Table III. It should be kept in mind that the reliability of experimental single-ion heats and volumes of solution are adversely affected by the need for some assumptions in separating the cationic and anionic contributions.[4b]

An experimental ΔV°_{sol} of −17 ± 2 cm^3/mol or −28.4 ± 3 Å^3 per ion has been reported for Na^+ in methanol.[31a] In addition, the volume of solution for CH_3ONa in methanol extrapolated to infinite dilution was determined to be −4.3 cm^3/mol or −7.2 Å^3 per ion pair assuming complete dissociation.[31b] Combining these results an estimate of 21 ± 3 Å^3 can be made for the ΔV°_{sol} of methoxide ion in methanol. It may also be noted that in water ΔV°_{sol}'s for Na^+, Cl^-, and OH^- are −11, −39, and 2 Å^3 per ion.[30] The computed results for Na^+ and CH_3O^- in methanol recorded in Table III are in accord with the experimental data, though the error bars for the computed numbers are large (ca. ±120 Å^3). Half the uncertainty comes from the volume for the pure liquid which could be improved in a longer simulation. Incidentally, the computed density of the pure solvent (0.743 g cm^{-3}) is close to the experimental value (0.787).[7b]

The heat capacities (C_p),isothermal compressibilities (κ), and coefficients of themal expansion (α) have also been computed for the pure liquid and the two solutions. Since these quantities are obtained from fluctuation formulas,[7b,8,9] the error bars are so large that no conclusions can be reached concerning the changes upon dissolving the ions; all quantities overlap. Further study with very long runs is needed to examine the convergence of these fluctuation properties in NPT simulations as was done for C_V in NVT calculations.[32]

Summarizing this section, the computed heats and volumes of solution are in accord with the available experimental data; however, improvements in the precision of the theoretical results are desirable.

(25) Choux, G.; Benoit, R. L. *J. Am. Chem. Soc.* **1969**, *91* 6221.
(26) Bartmess, J. E.; Scott, J. A.; McIver, R. T. *J. Am. Chem. Soc.* **1979**, *101*, 6046, 6056.
(27) Alexander, D. M.; Hill, D. J. T. *Aust. J. Chem.* **1969**, *22*, 347.
(28) Arshadi, M.; Kebarle, P. *J. Phys. Chem.* **1970**, *74*, 1483.
(29) Rossini, F. D.; Knowlton, J. W.; Johnston, H. L. *J. Res. Natl. Bur. Std.* **1940**, *24*, 369.
(30) Friedman, H. L.; Krishnan, C. V. In ref 4a, p 1.
(31) (a) Kawaizumi, F.; Zana, R. *J. Phys. Chem.* **1974**, *78*, 627. (b) Schwitzgebel, G.; Barthel, J. *Z. Phys. Chem. (Frankfurt am Main)* **1979**, *68*, 79.
(32) Mezei, M.; Swaminathan, S.; Beveridge, D. L. *J. Chem. Phys.* **1979**, *71*, 3366.

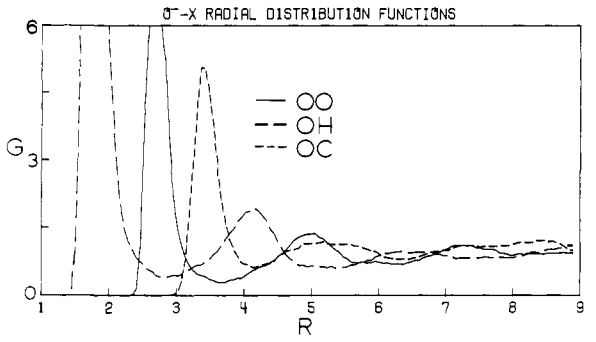

Figure 3. Computed rdfs between O in CH_3O^- and the O, H_O, and C atoms in the methanol solvent molecules.

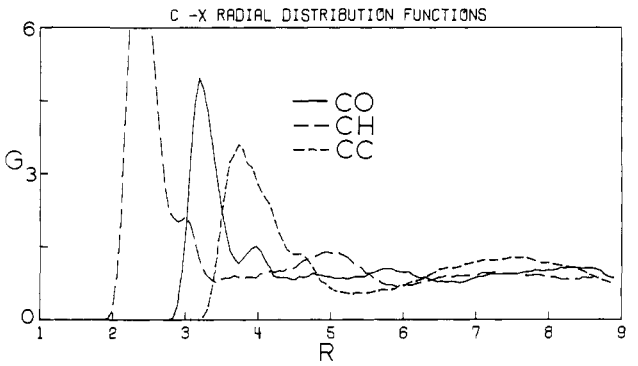

Figure 4. Computed rdfs between the C in CH_3O^- and the O, H_O, and C atoms in the methanol solvent molecules.

B. Solute–Solvent Structure. The solute–solvent radial distribution functions (rdfs) are shown in Figure 2 for Na^+ and in Figures 3 and 4 for CH_3O^-. For Na^+, the distributions indicate the presence of three relatively well-defined solvent layers. The first peaks in the NaO, NaH, and NaC rdfs all integrate to exactly six solvent molecules in the first shell. This is the same value as for the coordination number of Na^+ in water obtained in Mezei and Beveridge's Monte Carlo calculation[14] and in X-ray diffraction studies of dilute aqueous solutions of $NaBF_4$.[6,33] In addition, coordination numbers of 5–6 for Na^+ in methanol have been derived from mobility measurements via Stokes' law, though the interpretation of results from this method is controversial.[5a,34] The maximum for the first peak in the NaO rdf (Figure 2) occurs at 2.32 ± 0.03 Å which is also similar to the NaO distances of 2.38 and 2.4 Å found for sodium ion in water from X-ray data.[6,33]

Interestingly, the well-resolved second peak in the NaO rdf for the methanolic solution also integrates to six solvent molecules. This contrasts conventional ideas about the buildup of solvent shells with increasing numbers of solvent molecules in each layer. The reason for the discrepancy stems from the substantial compression of the first solvent shell. The extremity of the first shell can be esimated at about 4.2 Å which is the position of the first minimum in the NaC rdf, although from Figure 2 it is apparent that there is some overlap of second-shell oxygens with first-shell methyls and hydrogens. The volume of the first shell is then roughly 310 $Å^3$ which is 120 $Å^3$ less than the volume occupied by six methanol molecules in the pure liquid. Thus, substantial compression occurs in the first solvent shell, while similar computations indicate the density is near normal beyond the first shell. Additional evidence that the solute's influence is much diminished beyond the first shell is presented in the next section. Thus, the solvent–solvent interactions are dominant outside the first shell and establish a density close to that for the pure liquid. It follows that the occurrence of a similar number of solvent molecules in the first two shells results from the drive to compress the first shell and to achieve a near-normal density beyond it.

(33) Ryss, A. I.; Radchenko, I. V. *J. Struct. Chem.* **1964**, *5*, 489.
(34) Ulich, H. *Trans. Faraday Soc.* **1927**, *23*, 388.

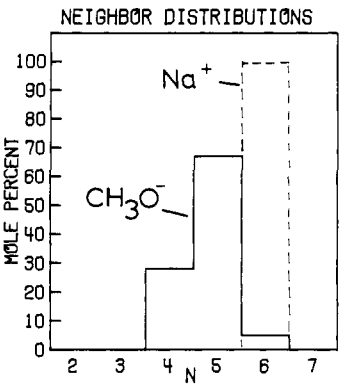

Figure 5. Distributions of solvent molecules within the range of the first peak in the NaO rdf for Na^+ in methanol and the O^-O rdf for CH_3O^- in metanol.

The rdfs for the methoxide oxygen in Figure 3 reveal at least two solvent layers with the hydrogens in the first shell closest to the ion as expected. The first peaks in the OH, OO, and OC rdfs integrate to an average of about five nearest neighbors for the oxygen. There are no closely related experimental data, though coordination number of 6 for both OH^- and Cl^- in water from diffraction results can be quoted.[6] Integration to the second minima in the OH and OO rdfs indicates roughly eight molecules in the second layer around oxygen in the ion. The analysis for methoxide is complicated by the rdfs for the methyl group in Figure 4 which reveal sharp first peaks closely followed by secondary maxima. The first peaks for the CH and CO rdfs integrate to five solvent molecules which can be assigned as the same ones nearest the oxygen in the ion; the shift in the peak positions shows the five solvent molecules are about 0.5 Å farther from the methyl carbon than from the oxygen in CH_3O^-. On the other hand, the secondary maxima contain one to two solvent molecules which from the peak positions are nearer the methyl group and directed toward it hydrogens first. Thus, the notion of solvent shells is not as well defined for the nonspherical methoxide ion as for Na^+ in methanol. The picture that emerges is for a layered arrangement with five solvent molecules strongly coordinated to the oxygen, followed by two more associated with the methyl group, and then a second partial shell of five to six molecules near the oxygen end of CH_3O^-. A distinct second layer for the methyl group is not clearly defined by the rdfs in Figure 4. The maximum near 5 Å in the CH rdf can be attributed to the second partial shell nearer the oxygen.

In order to check if the coordination numbers of 6 and 5 for Na^+ and O in CH_3O^- are static or the average of a distribution, the distributions for neighbors within the range of the first peaks of the NaO and OO rdfs were constructed. Such analyses are made after the runs from configurations saved at intervals of 2.5K. The results are presented in Figure 5 where it is seen that only 6 coordination is found for Na^+, while more geometric variety is apparent near the O in CH_3O^-. The data also imply that exchange of solvent molecules in and out of the first shell was slight in the run for Na^+, but more common for methoxide. This is supported by the NaO rdf where the minimum between the first two shells has a magnitude near zero (0.005).

Many of the structural notions in this section can be reinforced with stereoplots of actual configurations. Examples are provided in Figures 6 and 7 where representative configurations are illustrated. For clarity, only the 12 solvent molecules nearest the Na^+ or O in CH_3O^- are shown. The Na^+ in Figure 6 has six nearest neighbors in a roughly octahedral arrangement. Five of these are clearly hydrogen bonded to molecules in the second shell, so hydrogen bonding has an important influence on the orientation of monomers in the second shell. The remaining molecule in the second shell for this configuration is at the top of the figure and is hydrogen bonded to a second-shell neighbor.

Most of the solvent molecules in Figure 7 are clustered near the oxygen end of the methoxide ion. Five are coordinated directly to the oxygen with the methyl group forming the missing vertex

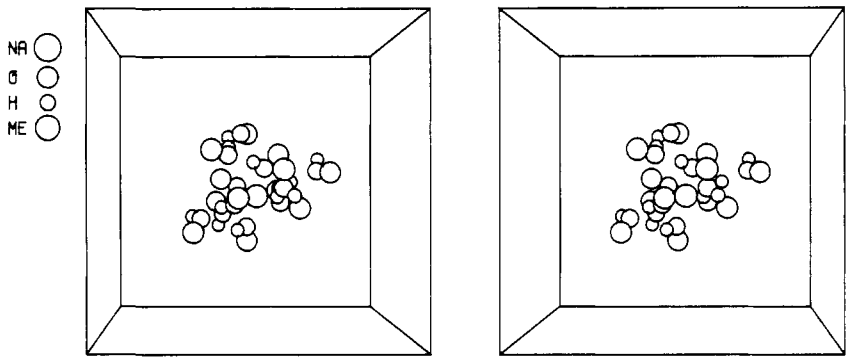

Figure 6. Stereoplot showing the 12 solvent molecules nearest the ion from one configuration in the simulation of Na^+ in methanol.

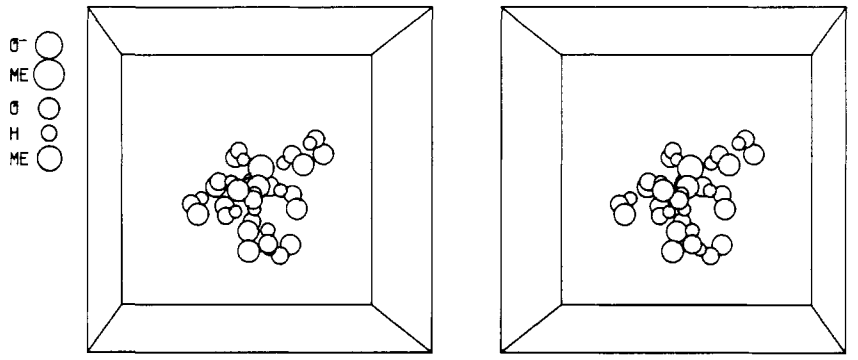

Figure 7. Stereoplot showing the 12 solvent molecules nearest the O^- in CH_3O^- from one configuration in the simulation of CH_3O^- in methanol.

of an octahedron. Another five corresponding to the second shell are hydrogen bonded to the first five. The remaining two monomers are in the upper right of the figure. One seems to be coordinating more with the methyl group than the oxygen of the ion and is undoubtedly part of the second maximum at a distance of ca. 4 Å in the CO rdf (Figure 4). The last molecule is hydrogen bonded to the previous one and could also be in the second maximum.

C. Solute–Solvent Energetics. The total bonding energy distributions for the solutes are reported in Figure 8. Both distributions are unimodal and show that the ions experience a continuum of energetic environments covering ca. 40 kcal/mol ranges. Grossly different alternate environments for the ions could lead to multiple maxima in such plots. The present results are consistent with a thermal distribution over one basic environment for each ion.

The energy pair distributions for the ion–solvent interactions are illustrated in Figure 9. The low-energy bands are due to the solvent molecules in the first shells and integrate to 6.0 and 4.6 for Na^+ and CH_3O^-. The spikes near 0 kcal/mol are associated with the many interactions between the ions and distant solvent molecules including those beyond the 10-Å cutoff. Additional interesting features are apparent near -6 kcal/mol in both distributions. These shoulders may be assigned to the solvent molecules in the second shells which shows solute–solvent interactions beyond the first shell are not much stronger than solvent–solvent hydrogen bonding. Thus, the difference in bonding between the solvent and the ions in the first two shells is pronounced, particularly for Na^+ where the interaction with the second-shell molecules is about 20 kcal/mol weaker than for the coordination sphere. This is further emphasized by noting that intergration of the low-energy peak in Figure 9 reveals that over 70% of the Na^+–solvent bonding (E_{SX}) comes from the first solvent shell. In addition, integration of the high-energy tail of the distribution shows that the Na^+ actually has repulsive interactions with 16 of the ca. 60 solvent molecules within 10 Å. Consequently, as alluded to in the last section, the solvent–solvent interactions, especially because there are so many of them, apparently control the solvent orientation and density beyond the first shell.

D. Solvent Structure. The OO, OH, and HH rdfs for the solvent molecule pairs are shown in Figure 10 and the CC, CO,

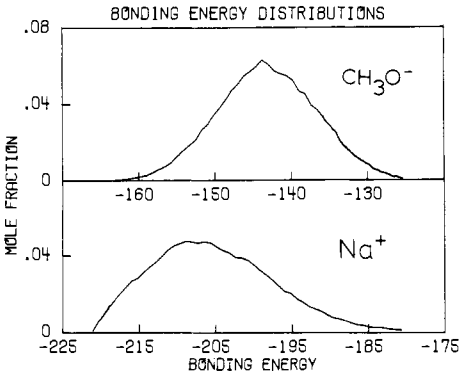

Figure 8. Computed solute–solvent bonding energy distributions for Na^+ and CH_3O^- in methanol. The ordinate gives the mole fraction of solutes with the bonding energy shown on the abscissa. Units for the ordinate are mole fraction per kcal/mol.

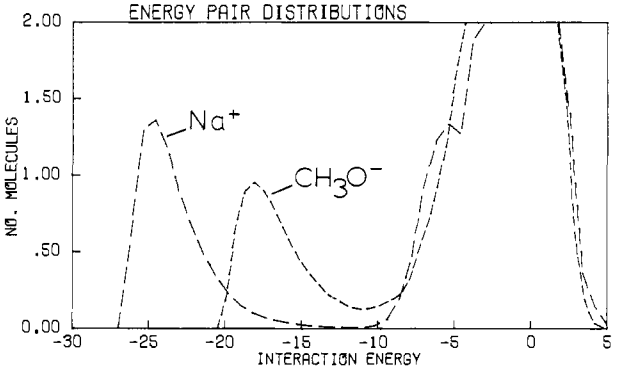

Figure 9. Computed solute–solvent energy pair distributions for Na^+ and CH_3O^- in methanol. The ordinate records the number of solvent molecules bound to the ion with the energy given on the abscissa. Units for the ordinate are molecules per kcal/mol.

and CH rdfs are in Figure 11. The corresponding rdfs for the pure liquid at 25 °C and 1 atm are given for comparison.[7b] The structure of pure liquid methanol has been described at length

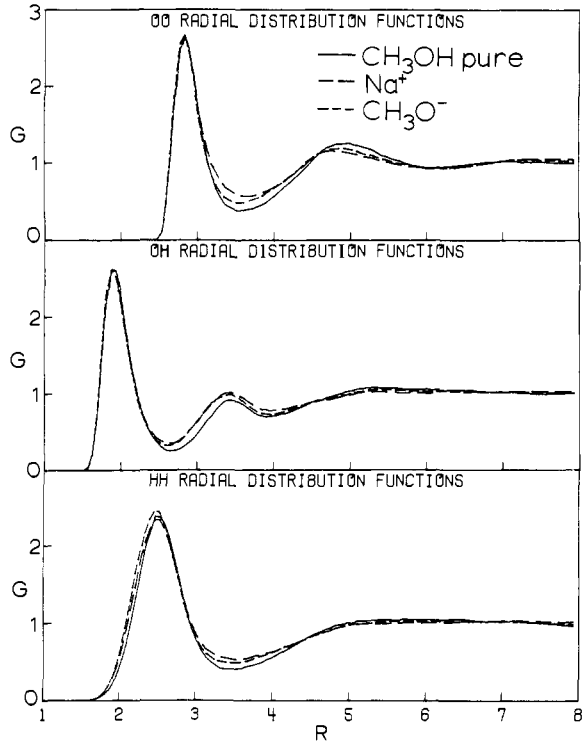

Figure 10. Computed OO, OH, and HH rdfs between solvent molecules for pure methanol and for the solutions of Na^+ and CH_3O^- in methanol.

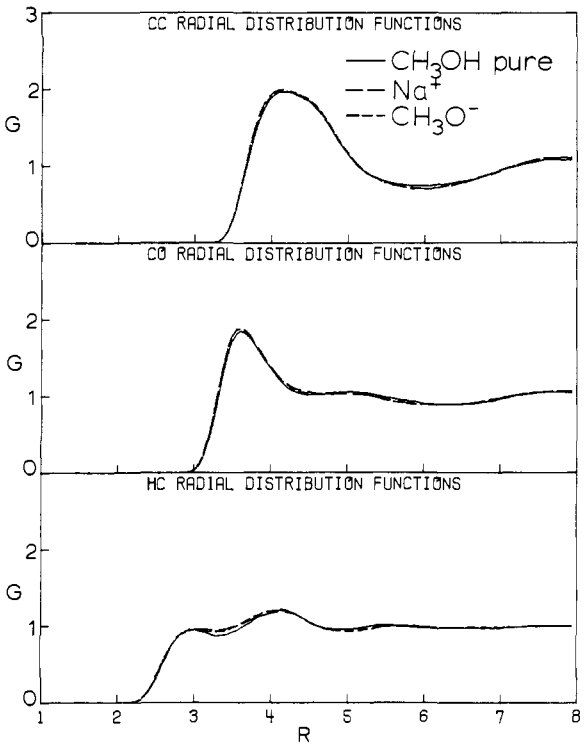

Figure 11. Computed CC, CO, and CH rdfs between solvent molecules for pure methanol and for the solutions of Na^+ and CH_3O^- in methanol.

previously, so the earlier work can be consulted for details.[7,35] Briefly, the liquid consists of winding hydrogen-bonded chains. The average number of hydrogen bonds per monomer is near 2; however, only 60–70% of the monomers are in exactly two hydrogen bonds. Most of the remainder participate in one or three hydrogen bonds corresponding to chain ends and branch points (Y junctions). The first peaks in the OO, OH, HH, and CH rdfs are due to the hydrogen-bonded neighbors. The other peaks at short distance in the rdfs also include some contributions from beyond the nearest neighbors.

As witnessed in Figures 10 and 11, introduction of the ions has little effect on the solvent structure as measured by the rdfs. It should be realized that the five or six solvent molecules strongly bound to the ions only represent about 5% of the total number of solvent molecules, so their influence on the computed rdfs is small. The slight shifting in of the second peaks in the OO and OH rdfs is consistent with the occurrence of some compression,[7b] though the effect is not apparent in the rdfs involving the methyl group (Figure 11). The constancy of the first peaks in the rdfs also indicates that the hydrogen bonding in the solvent is perturbed little by the ions (vide infra).

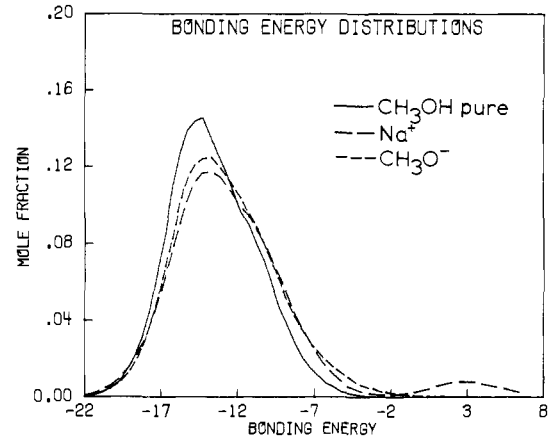

Figure 12. Computed solvent–solvent bonding energy distributions for pure methanol and for the solutions of Na^+ and CH_3O^- in methanol. The ordinate records the mole fraction of solvent molecules bound to other solvent molecules with the total bonding energy given on the abscissa. Units for the ordinate are mole fraction per kcal/mol.

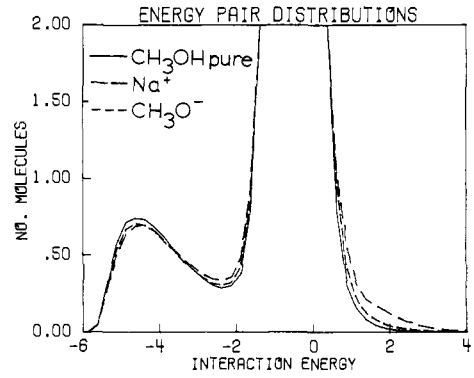

Figure 13. Computed solvent–solvent energy pair distributions for pure methanol and the solutions of Na^+ and CH_3O^- in methanol. The ordinate records the number of solvent molecules bound to another solvent molecule with the energy given on the abscissa. Units for the ordinate are molecules per kcal/mol.

E. Solvent Energetics and Hydrogen Bonding. The total solvent–solvent bonding energy distributions for the solutions and the pure liquid are presented in Figure 12. Although the curves are similar, the results for the dilute solutions are skewed to higher energy. In fact, the Na^+ results show a second small peak near +3 kcal/mol. Not surprisingly, this peak contains about 6 of the 127 molecules. Thus, the solvent monomers in the first shell around Na^+ repel each other enough to show no net solvent–solvent bonding. Similarly, the skewing of the results for CH_3O^- to higher energy also indicates weak solvent–solvent bonding for the solvent molecules strongly bound to the ion.

The energy pair distributions for the solvent–solvent interactions are given in Figure 13. Again the only substantial differences occur at high energy where more repulsive solvent–solvent interactions are found in the solutions than in the pure liquid. The repulsion between monomers in the first shell around Na^+ is the most pronounced since the stronger ion–solvent interactions yield

(35) Jorgensen, W. L. *J. Am. Chem. Soc.* **1980**, *102*, 543.

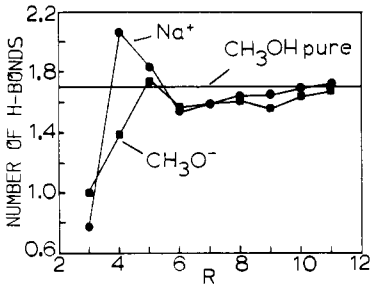

Figure 14. The average number of hydrogen bonds for each solvent molecules as a function of distance from the ions in the methanolic solutions of Na^+ and CH_3O^-. The solid line at 1.7 is the average number of hydrogen bonds calculated for monomers in pure liquid methanol.

more compression and less separation of the solvent molecules. The peaks at low energy in these distributions are for the hydrogen-bonded neighbors. Integration to the minimum at −2.375 kcal/mol yields an average of 1.6–1.7 hydrogen bonds per monomer in each case. This figure is clearly sensitive to the integration limit at discussed previously.[7]

In order to obtain more information on the effect of the ions on the liquid's structure, thorough analyses of the hydrogen bonding in the solutions were carried out. The usual energetic definition of a hydrogen bond obtained from the position of the minimum in the energy pair distribution was used; i.e., any pair of solvent molecules with an interaction energy below −2.375 kcal/mol is considered to be hydrogen bonded.[36] The hydrogen bonding was studied as a function of distance from the Na^+ and O in CH_3O^- by obtaining separate averages for the first shell (0–3.5 Å) and for each 1 Å thick shell between 3.5 and 11.5 Å from the ions.

A key result is displayed in Figure 14 which shows the average number of hydrogen bonds per solvent molecule as a function of distance from the ions. The solid line at 1.7 hydrogen bonds is the value for the pure liquid. For Na^+, the solvent molecules in the first shell have NaO distances around 2–3 Å and are found to participate in an average of 0.8 hydrogen bond each, primarily via their hydrogens to oxygens in the second shell (Figure 6). In the second shell (3.5–5.5 Å), the average number of hydrogen bonds is significantly greater than in the pure solvent. Thus, these molecules are oriented efficiently to hydrogen bond not only to the first-shell molecules but also to each other and outer neighbors. Beyond the second shell, the average number of hydrogen bonds gradually increases from 1.6 at 6 Å to the bulk value of 1.7 at 10 Å. Though this suggests structure breaking, the effect is slight, particularly in view of the error bars of ca. ±0.05 for the hydrogen-bond numbers.

For methoxide ion, the first group of five neighbors occurs at OO distances of 2.5–3.5 Å (Figure 3). These molecules are found to participate in exactly one hydrogen bond each as hydrogen-bond acceptors for hydroxyl hydrogens in the second layer (Figure 7). Again, the second-shell molecules (4.5–5.5 Å) show enhanced hydrogen bonding though not as pronounced as for sodium ion. The hydrogen-bonding profiles beyond the second shell are very similar for both ions and are consistent with mild structure breaking.

The key point is that all the evidence indicates that outside the first shells liquid methanol easily accomodates the ions. The interfacial B region proposed by Frank and Wen for aqueous electrolyte solutions is not clearly evident for the methanolic solutions. This requires facile interfacing of the first solvent shell (the A region) to the bulk solvent which can be rationalized as follows. The ions cause compression and orientation of the first-shell molecules so that there is a protrusion of hydroxyl hydrogens (Na^+) or oxygens (CH_3O^-) readily available for hydrogen bonding to the bulk solvent. Methanol is not as structured as water so this interfacing is facile. In simple terms, a water monomer desires four hydrogen bonds and it has four sites for these bonds, the two hydrogens and the two lone pairs. This allows water less flexibility in hydrogen bonding to the first shell than methanol which only needs two hydrogen bonds and has three sites, the hydroxyl hydrogen and lone pairs. It may be noted that the presence of more extensive interfacial regions for aqueous electrolyte solutions is supported by the common occurrence of negative B viscosity coefficients, whereas only positive values are found in methanol.[4,5a] Friedman and co-workers have also concluded that "the structure-broken region is absent or at least much smaller in methanol" based on the relatively small solvent isotope effects on ΔH_{tr} between CH_3OH and CH_3OD vs. H_2O and D_2O for alkali cations.[30] The influence of the ions on the outer solvent structure in methanol is primarily indirect via orientation of the hydroxyl hydrogens or oxygens outward from the first shell. Beyond the first shell, the ions' influence is not enough to significantly diminish the hydrogen bonding in the solvent. In fact, the hydrogen bonding for molecules in the second solvent shell is somewhat enhanced.

Several other distributions were obtained for the hydrogen bonds including those for the hydrogen-bond angles and the Coulomb and Lennard-Jones contributions to the hydrogen-bond energies.[7] In each case, the results were the same within the statistical limits as for the pure solvent independent of the distance from the ions. This states that the hydrogen bonds in the solutions have not been distorted geometrically or energetically by the presence of the ions.

IV. Conclusion

The present calculations illustrate the potential for Monte Carlo simulations to yield detailed insights into the structures and properties of nonaqueous solutions. Such information should be of great utility in furthering the understanding of organic chemistry in solution and of the molecular origin of solvent effects on reactivity. Some technical issues concerning effects of system size, boundary conditions, and three-body interactions warrant further investigation. In addition, the statistical uncertainties in the computed thermodynamic properties of solution may be problematic for some potential applications. Specifically, it would be difficult with current procedures to obtain heats and volumes of solution for individual species to within ±5 kcal/mol and ±50 $Å^3$. Thus, studying solvent effects involving differences in heats of solution for two species of less than ca. 10 kcal/mol is currently impractical.

An important finding from the simulations is the small influence of the ions on the solvent beyond the first shell. The facile interfacing of the first shell to the bulk for methanol contrasts the useful three-region model for aqueous electrolyte solutions. An interesting consequence of the compression of the first shell by Na^+, but near bulk density beyond it, is that the second solvent layer contains the same number of solvent molecules as the coordination sphere.

Acknowledgment. Gratitude is expressed to the National Science Foundation (CHE80-20466) for support of this study and to the CNRS-NSF exchange program for a fellowship granted to B.B.

Registry No. Na^+, 17341-25-2; CH_3O^-, 3315-60-4; CH_3OH, 67-56-1.

(36) An interesting paper has appeared that considers the effects of averaging over librational motion in hydrogen-bonding analyses for water. The librational averaging is not very significant for energetic definitions of a hydrogen bond as lenient as applied in our work. See: Hirata, F.; Rossky, P. J. *J. Chem. Phys.* **1981**, *74*, 6867.